



First Optical Hyperfine Structure Measurement in an Atomic Anion

A. Fischer, C. Canali, U. Warring, and A. Kellerbauer*

Max Planck Institute for Nuclear Physics, Saupfercheckweg 1, 69117 Heidelberg, Germany

S. Fritzsche[†]

GSI Helmholtzzentrum für Schwerionenforschung GmbH, Planckstraße 1, 64291 Darmstadt, Germany

(Received 17 December 2009; published 18 February 2010)

We have investigated the hyperfine structure of the transition between the $5d^7 6s^2 4F_{9/2}^e$ ground state and the $5d^6 6s^2 6p 6D_9^o$ excited state in the negative osmium ion by high-resolution collinear laser spectroscopy. This transition is unique because it is the only known electric-dipole transition in atomic anions and might be amenable to laser cooling. From the observed hyperfine structure in $^{187}\text{Os}^-$ and $^{189}\text{Os}^-$ the yet unknown total angular momentum of the bound excited state was found to be $J = 9/2$. The hyperfine structure constants of the $4F_{9/2}^e$ ground state and the $6D_{9/2}^o$ excited state were determined experimentally and compared to multiconfiguration Dirac-Fock calculations. Using the knowledge of the ground and excited state angular momenta, the full energy level diagram of $^{192}\text{Os}^-$ in an external magnetic field was calculated, revealing possible laser cooling transitions.

DOI: 10.1103/PhysRevLett.104.073004

PACS numbers: 32.80.Gc, 32.30.Bv, 32.70.Cs, 37.10.Rs

Laser cooling is a technique proposed more than three decades ago for the cooling of particle ensembles in beams or particle traps [1,2]. It is based on the directional absorption of photons and their isotropic reemission, resulting, on average, in a deceleration of the resonantly excited particles. While the laser cooling of positive atomic ions [3,4] and neutral atoms [5] is today commonplace and has opened the avenue for exciting new fields such as particle condensation [6] and ion crystals [7], it has not yet been demonstrated for negative atomic ions. This shortcoming is due to the unique binding mechanism of the valence electron in atomic anions, which is fundamentally different from that in other atomic systems. In marked contrast to cations and neutral atoms, the binding of the excess electron relies heavily on electron-electron correlation effects. The additional electron in the outermost shell causes all other electrons to adjust their motions in order to minimize the overlap of their wave functions according to electrostatic repulsion (Coulomb correlation) and Pauli's exclusion principle (exchange correlation) so that the whole system gains enough potential energy to be stable.

The correlation effects, though essential for all negative ions, are reduced if one of the electrons is excited and basically moves around a neutral atomic core. Therefore, excited bound states are rare in negative ions, and where they occur they were found to have almost always the same parity as the ground state [8]. This means, however, that transitions between these levels are electric-dipole ($E1$) forbidden and that the upper state is difficult to excite. An exception to this empirical rule was experimentally found only very recently in the transition metal osmium [9]. Using infrared laser photo detachment spectroscopy, Bilodeau and Haugen discovered an excited bound state with opposite parity with respect to the $4F_{9/2}^e$ ground state,

making a strong $E1$ transition between them possible. The presence of such a transition, previously thought not to exist in atomic anions, is a prerequisite to studying the atomic system by optical spectroscopy. It also paves the way for the cooling of atomic anions by laser interaction for the first time [10].

In a previous article, first results of collinear laser spectroscopy on this transition in $^{192}\text{Os}^-$ (natural abundance 41%) were presented [11]. They confirmed that there is indeed a dipole transition between the two states. The transition frequency was found to be $\nu_0 = 257.831\,190(35)$ THz and the Einstein coefficient $A_E = 330(110)$ s⁻¹, corresponding to an observed cross section of $\sigma = 2.5(7) \times 10^{-15}$ cm² at a Doppler-broadened linewidth of $\Gamma = 45$ MHz. In this Letter, we report the resolved hyperfine structure (HFS) of Os^- and its consequences for the laser cooling of negative ions in a Penning trap. For this purpose, we have performed high-resolution laser spectroscopy on $^{187}\text{Os}^-$ (natural abundance 1.6%) and $^{189}\text{Os}^-$ (natural abundance 16%), the only stable osmium isotopes with a nonvanishing nuclear spin, and we determined the HFS constants of the ground state and the $6D_9^o$ excited state. These experimental data represent the first-ever optical HFS measurements in any atomic anion. From the observed hyperfine splitting the yet unknown total angular momentum of the excited state was deduced. This also enabled us to predict the Zeeman splitting of the $E1$ transition in an external magnetic field and identify a suitable transition for Os^- laser cooling.

The experimental setup has been described in detail elsewhere [11]. The ions are produced in a Middleton-type negative-ion sputter source [12] and are shaped to a beam with electrostatic lenses and quadrupoles. The produced ion beam contains all naturally occurring osmium

isotopes. It is mass separated in a dipole magnet and guided downstream into the spectroscopy region. There the beam is superimposed collinearly with a laser beam, which is provided by a tunable cw optical parametric oscillator system [13]. At the end of the spectroscopy region, an electrostatic deflector leads the ions into a Faraday cup. In forward direction neutralized particles are detected with a microchannel-plate detector. The neutralization of excited ions is achieved by a longitudinal electric field of up to $2 \times 10^6 \text{ V m}^{-1}$, which can be applied just before the deflector. The use of electric-field detachment enhances the detection efficiency by up to 2 orders of magnitude when compared to a photodetachment measurement and thus also allows the detection of weak resonances. Owing to the collinear configuration, all measured frequencies are Doppler shifted toward higher frequencies. The rest frame frequency of each resonance is obtained by measuring the shifted frequencies at different energies and fitting the data points to the Doppler shift function [11].

To analyze the HFS of the dipole transition in $^{187}\text{Os}^-$ and $^{189}\text{Os}^-$, their optical spectra around 1163 nm were recorded. Figure 1 shows the spectrum of $^{187}\text{Os}^-$. It contains four resonances: two weak ones that correspond to the $F = F' \pm 1$ transitions and two strong ones for $F = F'$. For the $^6D^o$ excited state, this uniquely constrains the angular momentum J_e since the four resonances arise from the coupling of the total electronic angular momentum J with the nuclear spin I to the total angular momentum F , with $|J - I| \leq F \leq J + I$. Electric-dipole transitions between two multiplets are then subject to the standard selection rule $\Delta F = 0, \pm 1$. Therefore, the number of resonances depends on the quantum numbers J_g and J_e of the two states and the nuclear spin I . With the values $J_g = 9/2$ and $I(^{187}\text{Os}) = 1/2$ already known, exactly four transitions are only possible if $J_e = 9/2$, as for the ground state.

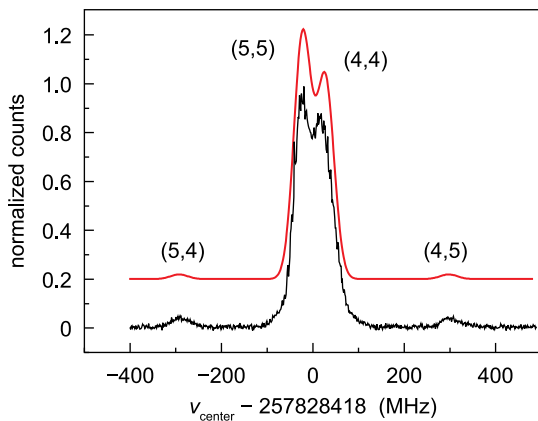


FIG. 1 (color online). Hyperfine structure of $^{187}\text{Os}^-$. The two strong resonances correspond to transitions with $F = F'$ and the two weak ones to transitions with $F = F' \pm 1$. The red (upper) line shows a calculated spectrum consisting of a superposition of four Gaussian curves with the theoretical relative intensities.

Similarly, Fig. 2 displays the measured spectrum of $^{189}\text{Os}^-$. In this case the spectrum consists of ten resonances in total: four strong and six weak ones. Following the same arguments as above, we find these ten resonances again consistent with $J_e = 9/2$. The spectra in Figs. 1 and 2 were fitted with a superposition of four and ten Gaussian curves, respectively, leaving the peak center frequencies and intensities as free parameters. To determine the HFS constants, the Casimir formulas [14] were used:

$$\Delta E^{\text{res}} = E_F^{\text{excited}} - E_{F'}^{\text{ground}} \quad (1)$$

$$E_F = E_J + \frac{A}{2}C + \frac{B}{2}D \quad (2)$$

$$C = F(F + 1) - I(I + 1) - J(J + 1) \quad (3)$$

$$D = \frac{\frac{3}{4}C(C + 1) - I(I + 1)J(J + 1)}{I(2I - 1)J(2J - 1)}, \quad (4)$$

where A and B are the magnetic-dipole ($M1$) and the electric-quadrupole ($E2$) HFS constants, respectively, and E_J is the center-of-gravity energy of the multiplet.

From Eq. (1) one obtains a system of equations, one for each of the possible transitions. There are four equations for three unknowns in the case of $^{187}\text{Os}^-$ and ten equations for five unknowns in the case of $^{189}\text{Os}^-$. To solve the system it is necessary to assign the measured transition frequencies to the corresponding equations, which is done by means of the characteristic intensities. The relative intensities of the hyperfine components only depend on the quantum numbers of their ground and excited states and can therefore be calculated once the HFS is known. The theoretical intensities were taken from the tables of White and Eliason [15] and are based on formulas first derived by Kronig [16] and Russell [17].

Using this procedure, however, the transition $F_1 \rightarrow F_2$ has the same intensity as $F_2 \rightarrow F_1$. Hence, only transitions with $F = F'$ can be clearly assigned to the measured frequencies. For all other transitions, there are two differ-

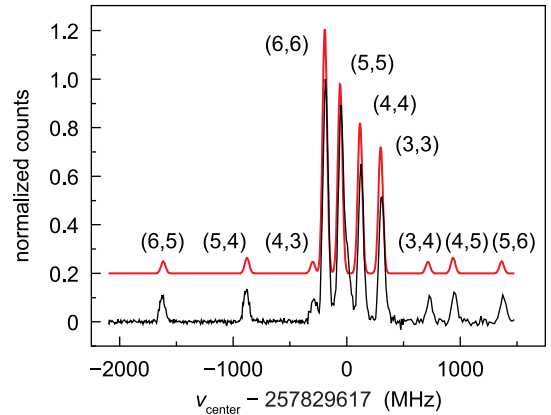


FIG. 2 (color online). The same as Fig. 1, but for $^{189}\text{Os}^-$.

ent possibilities. This gives rise to two systems of equations and consequently also to two sets of HFS constants. The possible results are displayed in Table I. In this procedure, the precision of the center-of-gravity frequencies is mainly limited due to uncertainties of the frequency measurement. The used wave meter has an uncertainty of 30 MHz if applied for an absolute frequency measurement. In addition, the recorded resonances are slightly asymmetric, which causes an additional systematic error of 5 MHz [11]. In contrast, the determination of the HFS constants is only based on the relative positions of the resonances. Therefore, the resulting uncertainty is much smaller, especially in the case of the HFS, where the single resonance frequencies are close to each other. The systematic uncertainty due to the wave meter drift during the measurements is estimated to be 3 MHz.

Because the measurements alone cannot determine the correct set of HFS constants, extensive multiconfiguration Dirac-Fock (MCDF) calculations have been carried out for the ${}^4F_{9/2}^e - {}^6D_{9/2}^o$ transition and its hyperfine structure. These computations were built on a systematic increase of the wave functions to include expansions up to a size of $\approx 50\,000$ configuration state functions in order to ensure that (at least) the major correlations in the electronic structure of the Os anion has been captured successfully. Not much needs to be said here about the MCDF method which has been found a versatile technique [18] to determine the energies and properties of atoms and ions with complex shell structures, including open d and f shells [19]. With the “best” approximation for the wave functions of the two lowest $J = 9/2$ levels, we obtained for the ${}^6D_{9/2}^o$ level an excitation energy of 0.95 eV (with regard to the ${}^4F_{9/2}^e$ ground state), in reasonable agreement with the 1.066 27 eV from experiment.

Using these wave functions, moreover, we obtained for the ${}^4F_{9/2}^e$ ground state the HFS constant $A = 299$ MHz which can be compared with the value $A = 386$ MHz from a previous computation by Norquist and Beck [20] and the experimental results from Table I. For the ${}^6D_{9/2}^o$ level, we obtained $A = 233$ MHz, which also agrees well with Set 1 of the hyperfine parameters from this table. We therefore conclude that Set 1 is the appropriate one for the isotope ${}^{189}\text{Os}^-$. From the constants for $A({}^{189}\text{Os}^-)$, we can also

identify the correct set for $A({}^{187}\text{Os}^-)$ since we have $A \propto \mu_I/I$ and

$$\frac{A({}^{189}\text{Os}^-)}{A({}^{187}\text{Os}^-)} = \frac{\mu_I({}^{189}\text{Os})I({}^{187}\text{Os})}{\mu_I({}^{187}\text{Os})I({}^{189}\text{Os})}, \quad (5)$$

where μ_I is the nuclear magnetic moment. The ratio of the magnetic moments is $\mu_I({}^{189}\text{Os})/\mu_I({}^{187}\text{Os}) = 10.2075(1)$ [21]. With the ground state splitting constant of ${}^{189}\text{Os}^-$, $A_g({}^{189}\text{Os}) = 216(2)$ MHz, Eq. (5) gives $A_g({}^{187}\text{Os}) = 63.5(6)$ MHz, supporting our conclusion that Set 1 is the correct one.

The details of the hyperfine splitting of the ${}^6D_{9/2}^o$ level can then be used to calculate and analyze the energy levels of ${}^{192}\text{Os}^-$ in an external magnetic field. The splitting of an atomic level in a magnetic field (Zeeman effect) results from the coupling of the magnetic moment of the atom or ion with the field \mathbf{B} . The interaction Hamiltonian is $\hat{H}_{\text{magn}} = \boldsymbol{\mu}\mathbf{B}$, where $\boldsymbol{\mu}$ is the total magnetic moment, composed of orbital and spin angular momentum contributions. The corresponding energy shift is

$$\Delta E_{\text{magn}} = g_J \mu_B M_J B, \quad (6)$$

where μ_B is the Bohr magneton, M_J the total angular momentum quantum number, and B the magnitude of the external magnetic field. The Landé factor g_J is given by

$$g_J = \frac{3}{2} + \frac{S(S+1) - L(L+1)}{2J(J+1)}. \quad (7)$$

Here we have assumed that the Russell-Saunders regime applies (LS coupling) and have furthermore set the electron g factor to its Dirac value $g_s = 2$. Inserting the quantum numbers of the ground and excited state determined above into Eq. (7), the Landé factors $g({}^4F_{9/2}) = 1.33$ and $g({}^6D_{9/2}) = 1.56$ are obtained.

With these values, the energy level diagram shown in Fig. 3 results. Using the appropriate selection rule $\Delta M_J = 0, \pm 1$, the transition is found to split into 28 allowed components, indicated by arrows in the figure. They are comprised of 10 π transitions, 9 σ^+ , and 9 σ^- transitions and have strengths that are proportional to the squares of the corresponding Clebsch-Gordan coefficients. For laser cooling we may tune the laser to the ${}^4F_{9/2} \rightarrow {}^6D_{9/2}$, $M_J = -9/2 \rightarrow -9/2$ transition, since it is one of the two strongest Zeeman lines available. We shall denote the corresponding frequency and transition rate with ν_c and Γ_c , respectively. Cooling from liquid-helium temperature (4.2 K) to the Doppler temperature requires the scattering of about 10^4 photons and takes about 200 s [10]. Prior to cooling, the transition line is Doppler broadened to ≈ 12 MHz.

TABLE I. Experimental $M1$ and $E2$ hyperfine structure constants for ${}^{187}\text{Os}^-$ and ${}^{189}\text{Os}^-$ (two sets each).

Nuclide		${}^4F_{9/2}^e$ HFS Constants (MHz)		${}^6D_{9/2}^o$ HFS Constants (MHz)	
		A	B	A	B
${}^{187}\text{Os}^-$	Set 1	64(2)	-	54(2)	-
	Set 2	-54(2)	-	-64(2)	-
${}^{189}\text{Os}^-$	Set 1	216(2)	396(4)	184(2)	479(4)
	Set 2	-184(2)	-479(4)	-216(2)	-396(4)

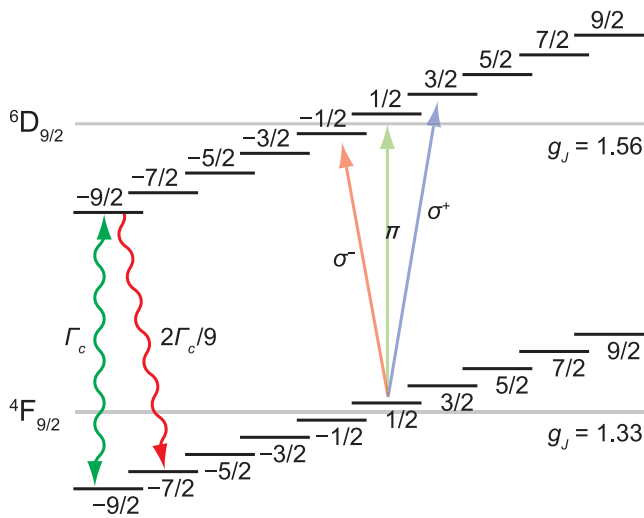


FIG. 3 (color online). Expected energy level diagram of $^{192}\text{Os}^-$ in an external magnetic field, based on calculated Landé factors. Wiggly arrows indicate the cooling transition (green vertical line) and the decay to a dark state (red slanted line). Straight arrows illustrate π , σ^- , and σ^+ transitions.

We can now estimate the efficiency of laser cooling at the $-9/2 \rightarrow -9/2$ subtransition. When the laser is tuned to this transition, the photons initially interact with $1/10$ of the ions, because the ground state is split into ten Zeeman levels. If we consider only allowed transitions, the excited ${}^6D_{9/2}$, $M_J = -9/2$ state can now decay back to the initial state with the spontaneous decay rate $\Gamma_c = A_E/(2\pi) = 53(18)$ Hz. In addition, it can also decay to the $M_J = -7/2$ Zeeman level of the ground state. Given the calculated intensities, the rate for that process is $2\Gamma_c/9$. The $M_J = -7/2$ Zeeman level of the intermediate ${}^4F_{7/2}$ state (see Ref. [9]) may also be populated. While the transition rate to that level is unknown, it can be calculated by considering that the rates scale roughly as $(\nu/\nu_c)^3$, for similar relative transition strengths. From the calculated binding energy for the intermediate state [20], it can be estimated to $\Gamma_c/33$. Both the ${}^4F_{9/2}$, $M_J = -7/2$ level and the ${}^4F_{7/2}$, $M_J = -7/2$ level are “dark” states which the cooling laser can no longer address. It is evident that these states will be populated well before significant cooling can occur. Hence, they will need to be repumped to the ${}^6D_{9/2}$, $M_J = -9/2$ state with two additional lasers. To prevent reheating during the repumping process, their bandwidths should be comparable to that of the cooling laser.

In conclusion, the hyperfine structure of the ${}^4F_{9/2} - {}^6D_{9/2}$ electric-dipole transition in the negative osmium ion was investigated by high-resolution optical spectroscopy. The measured constants are in reasonable agreement with the results of a theoretical analysis performed in the framework of the MCDF model. The total angular momen-

tum of the excited ${}^6D_{9/2}$ state, a crucial input for calculations of the expected Zeeman splitting in the external magnetic field of a Penning trap, was determined from the observed hyperfine transitions. Based on the resulting energy level diagram, suitable subtransitions for laser cooling were identified. In addition to the cooling laser, two other narrow-bandwidth lasers are required to repump those ions which decay to one of two “dark” states. Despite these technical issues, the present work strongly suggests that the first laser cooling of atomic anions is now within reach, paving the way for the production of ultracold samples of any negative ions.

This work was supported by the German Research Foundation (DFG) under Contracts No. KE1369/1-1 and No. FR1251/13-1. We thank the MPIK accelerator group and workshop, in particular, M. König, V. Mallinger, and M. Beckmann, for their invaluable support. The assistance of the group of S. Jochim for the wave meter calibration is gratefully acknowledged.

*To whom correspondence should be addressed.

a.kellerbauer@mpi-hd.mpg.de

†Also at: Department of Physical Sciences, P.O. Box 3000, 90014 University of Oulu, Finland.

- [1] T. W. Hänsch and A. L. Schawlow, *Opt. Commun.* **13**, 68 (1975).
- [2] D. Wineland and H. Dehmelt, *Bull. Am. Phys. Soc.* **20**, 637 (1975).
- [3] D. J. Wineland, R. E. Drullinger, and F. L. Walls, *Phys. Rev. Lett.* **40**, 1639 (1978).
- [4] W. Neuhauser, M. Hohenstatt, P. Toschek, and H. Dehmelt, *Phys. Rev. Lett.* **41**, 233 (1978).
- [5] S. Chu *et al.*, *Phys. Rev. Lett.* **55**, 48 (1985).
- [6] M. H. Anderson *et al.*, *Science* **269**, 198 (1995).
- [7] I. Waki, S. Kassner, G. Birkl, and H. Walther, *Phys. Rev. Lett.* **68**, 2007 (1992).
- [8] T. Andersen, *Phys. Rep.* **394**, 157 (2004).
- [9] R. C. Bilodeau and H. K. Haugen, *Phys. Rev. Lett.* **85**, 534 (2000).
- [10] A. Kellerbauer and J. Walz, *New J. Phys.* **8**, 45 (2006).
- [11] U. Warring *et al.*, *Phys. Rev. Lett.* **102**, 043001 (2009).
- [12] R. Middleton, *Nucl. Instrum. Methods* **214**, 139 (1983).
- [13] P. Groß *et al.*, *Opt. Lett.* (to be published).
- [14] H. Kopfermann, *Kernmomente* (Akademische Verlagsgesellschaft m.b.H., Frankfurt am Main, 1956), 2nd ed.
- [15] H. E. White and A. Y. Eliason, *Phys. Rev.* **44**, 753 (1933).
- [16] R. de L. Kronig, *Z. Phys.* **33**, 261 (1925).
- [17] H. N. Russell, *Nature (London)* **115**, 835 (1925).
- [18] I. P. Grant, in *Methods in Computational Chemistry*, edited by S. Wilson (Plenum Press, New York, 1988), Vol. 2, p. 1.
- [19] S. Fritzsche, *Phys. Scr.* **T100**, 37 (2002).
- [20] P. L. Norquist and D. R. Beck, *Phys. Rev. A* **61**, 014501 (1999).
- [21] A. Schwenk and G. Zimmermann, *Phys. Lett.* **26A**, 258 (1968).